

Comparative Study of Nonlinear Attitude Estimation in GNC Testbeds for Collegiate Self-Landing Rockets

Favour A. Adekola* and Anyi Xie Lin†
Georgia Institute of Technology, Atlanta, GA, 30332

When constructing a device that requires detail on its orientation in a 3D space, an inertial measurement unit (IMU) is a widely used solution. This commonly found sensor in the navigation space contains a gyroscope, accelerometer, and magnetometer, but two issues arise in IMUs when considering orientation calculation. The first is the natural noise generated from hardware electrical systems, and the second is the accumulated error when independently integrating a component into navigation equations. For instance, the double integration of noisy acceleration from the accelerometer produces an inaccurate estimate of our device's position, leading to a significant increase in error over time otherwise known as sensor drift. The solution is to utilize filters and algorithms that incorporate every part of the nine-axis IMU to help reduce noise from their components and avoid the problem of the previously mentioned drifting. Here we present the Complementary, Fourati, Extended Kalman Filter (EKF), Madgwick, and Mahony nonlinear estimation algorithms and compare their accuracy, when tuned, in predicting a predefined rocket path. We conclude that the Madgwick filter performed the best for our dataset, holding the smallest magnitude error. Using these results, we will proceed with the Madgwick filter in the development of our Monoprop UAV before implementing the algorithm into our rocket.

I. Nomenclature

θ	=	estimated attitude
θ_w	=	attitude estimated from gyroscope
θ_{am}	=	attitude estimated from the accelerometer and magnetometer
α	=	control parameter
x_t	=	state of system at time t
z_t	=	measurements at time t
P_t	=	estimated error covariance of the state after z_t
\hat{P}_t	=	predicted error covariance of the state before z_t
Q	=	process noise covariance
R	=	measurement noise covariance
f	=	nonlinear dynamic model function
h	=	nonlinear measurement model function
F	=	jacobian of f
H	=	jacobian of h
K_t	=	kalman gain at time t
I	=	identity matrix
q_t	=	attitude quaternion at time t
\hat{q}_t	=	estimated quaternion state
dt	=	time step
q_w	=	angular velocity quaternion
∇	=	gradient descent
$p(q)$	=	unitary pure quaternion of q
ω	=	attitude error

*GTPPL GNC sensing member, AIAA Undergraduate Student Member

†GTPPL GNC co-lead, AIAA Undergraduate Student Member

II. Introduction

IN fields like automotive, robotics, navigation, and aerospace, each underlying system must be fault-tolerant and reliable. For teams will face the significant costs of failed tests and missions. Accurate, automated, real-time measurements of a device's orientation relative to the Earth play a critical role in this process. The solution is to utilize an IMU divided into a gyroscope to measure angular velocity, an accelerometer to measure the velocity's rate of change, and a magnetometer to measure the strength and direction of a magnetic field. Because these devices suffer from noise and calibration errors when used outside of the nominal working conditions they are designed for, we consider filtering algorithms to enhance sensor accuracy for better attitude estimation. The filtering algorithms we explore and compare take the data from the IMU's gyroscope, accelerometer, and, sometimes, magnetometer, fuse their signals, and compute the attitude of the device. Specifically, this paper studies the Complementary, Fourati, Extended Kalman Filter (EKF), Madgwick, and Mahony algorithms and how well they perform for non-linear attitude estimations regarding our collegiate propulsive lander. These filters are being evaluated using a known trajectory and simulated sensor readings to understand the best choice for integration into the rocket test beds and further development of our Monoprop UAV.

III. Complementary Filter

Beginning with the Complementary filter, this simple filtering algorithm uses all 3 sensors of the IMU to estimate its current orientation. Two attitude estimates are generated: one from the gyroscope and one from the combined accelerometer and magnetometer data. One estimate is generated by tuning a weight for the average between the two, and that is then used to create the next state estimates.

Mathematically this is represented by:

$$\theta = \alpha\theta_w + (1 - \alpha)\theta_{am} \quad (1)$$

The controlling parameter, α , is also referred to as the filter gain and should be a decimal number within the range [0.0,1.0]. This value decides whether there is more trust in the gyroscope's readings versus the combined accelerometer and magnetometer readings.

Here is the output of the Complementary filter compared to the actual trajectory.

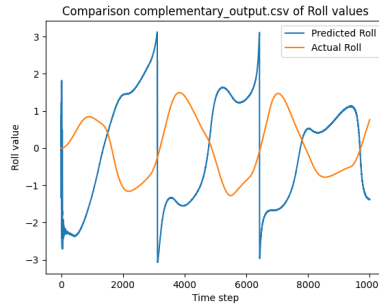


Fig. 1 Predicted roll values of the Complementary filter versus the actual roll values.

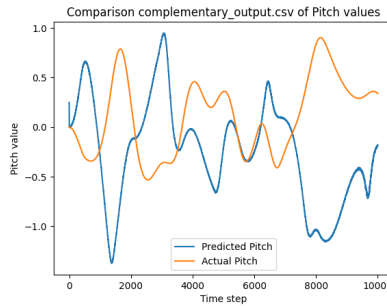


Fig. 2 Predicted pitch values of the Complementary filter versus the actual pitch values.

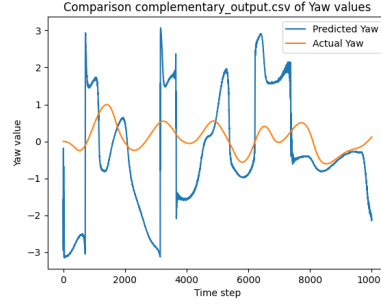


Fig. 3 Predicted yaw values of the Complementary filter versus the actual yaw values.

As mentioned, the Complementary Filter is a simple filtering algorithm, and with it comes a noticeable trade-off with the accuracy of its estimations. Looking at Fig.1-3, the filter produces estimations for attitude rarely following the true trajectory. Although it is computationally inexpensive, it suffers from being a relatively subpar attitude estimator when focusing on accuracy. Later in this paper, algorithms will be discussed that perform more accurately while utilizing the structure highlighted by the Complementary filter.

IV. Extended Kalman Filter

The Extended Kalman Filter is not an algorithm specifically for attitude estimation but rather a generalized approach for any non-linear system. In contrast with the Complementary filter, this filter is known to be computationally expensive, which could deter its usage in low-powered applications. The details of examining this difference in computational load are well analyzed in [1]. EKF utilizes a mathematical model of the system with states and their possible transitions to estimate where it will be in a time step using the previous state of the model and the measurements currently provided by the IMU. The algorithm functions in two steps: predict and update. The prediction step keeps an estimate of the state before the addition of the information provided by the current time step, and the update step refines this estimated state using the information provided by the IMU during the current time step. In this case, the states would refer to the attitude of the rocket.

The prediction step [2] can be represented using:

$$\hat{x}_t = f(x_{t-1}) \quad (2)$$

$$\hat{P}_t = F(x_{t-1})P_{t-1}F^T(x_{t-1}) + Q \quad (3)$$

The update step [2] can be represented using:

$$x_t = \hat{x}_t + K_t(z_t - h(\hat{x}_t)) \quad (4)$$

$$P_t = (I - K_tH_t(x_t))\hat{P}_t \quad (5)$$

Where the Kalman gain, K_t , is computed using:

$$K_t = \hat{P}_tH^T(\hat{x}_t)(H(\hat{x}_t)\hat{P}_tH^T(\hat{x}_t) + R) \quad (6)$$

One important thing to keep in mind about this filter is its usage of multiple processes like Jacobian calculations and matrix operations which often require relatively significant processing power to perform.

Here is the output of the Extended Kalman Filter compared to the actual trajectory.

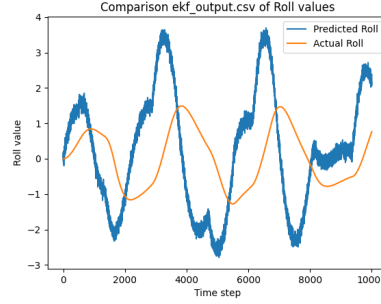


Fig. 4 Predicted roll values of the EKF versus the actual roll values.

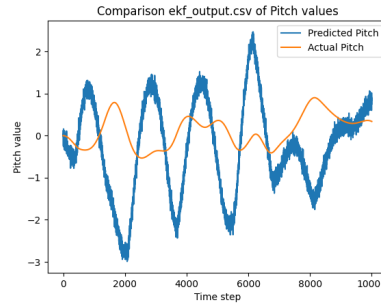


Fig. 5 Predicted pitch values of the EKF versus the actual pitch values.

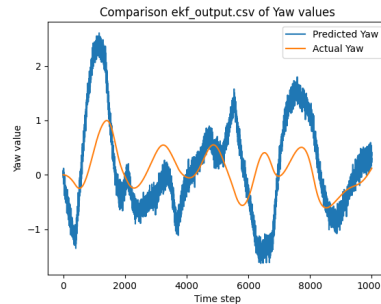


Fig. 6 Predicted yaw values of the EKF versus the actual yaw values.

V. Fourati Filter

Next, is a less commonly discussed filter among comparative studies. Fourati’s algorithm integrates data from all three sensors of the IMU: gyroscope, accelerometer, and magnetometer, using non-linear filtering techniques with the complementary structure to obtain an accurate estimate. The algorithm starts with an initial state estimate and predicts the projected attitude at the next time step using data from the gyroscope [3]. Then, this prediction is corrected for by accelerometer and magnetometer data, which refines the state estimate and sensor biases.

It is mathematically represented by:

$$q_t = q_{t-1} + \left(\frac{1}{2}\hat{q}q_{w,t}\right)dt \quad (7)$$

The Fourati filter ends up in the middle of the EKF and Complementary filter. It is not as expensive as the former, and it can be more reliable than the latter. That being said, the Fourati filter is not as widely used as the rest of the filters described in this paper, so there are fewer resources and documentation regarding its implementation.

Here is the output of the Fourati filter compared to the actual trajectory.

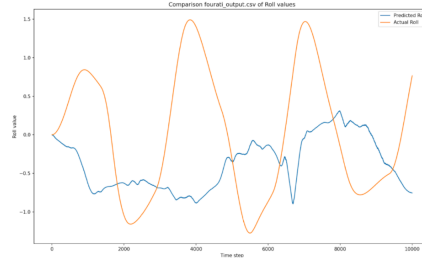


Fig. 7 Predicted roll values of the Fourati filter versus the actual roll values.

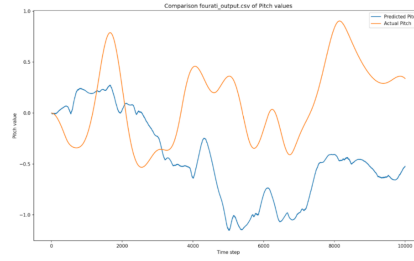


Fig. 8 Predicted pitch values of the Fourati filter versus the actual pitch values.

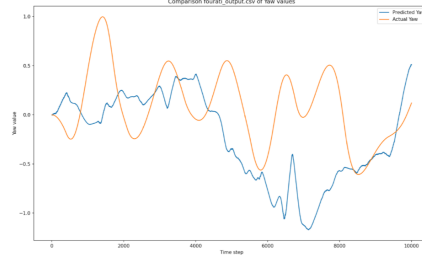


Fig. 9 Predicted yaw values of the Fourati filter versus the actual yaw values.

VI. Madgwick Filter

There are multiple variations of the Madgwick filter that rely on different combinations of the nine-axis IMU, but for this paper, we implemented a variation utilizing the entire IMU. The Madgwick filter minimizes the error created by raw gyroscope data by using the accelerometer and magnetometer to compute gyroscope measurement error with the gradient-descent algorithm [4]. This filter also implements the complementary structure. So, the computed error is integrated with the gyroscope readings to correct the estimation and provide the device's orientation.

This is mathematically described as:

$$q_t = q_{t-1} + (\dot{q}_{w,t} - \alpha \frac{\nabla f}{\|\nabla f\|})dt \quad (8)$$

The filter tuning parameter α is sometimes referred to as the gain and is referenced using β in other literature. The gradient descent of the objective function or dynamic model ∇f is what changes the most between the variations of the Madgwick filter and is elaborated in further detail by[4].

Here is the output of the Madgwick filter compared to the actual trajectory.

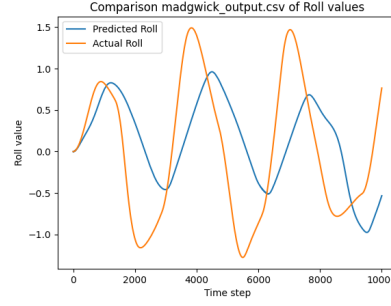


Fig. 10 Predicted roll values of the Madgwick filter versus the actual roll values.

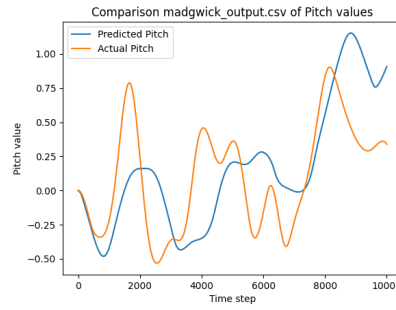


Fig. 11 Predicted pitch values of the Madgwick filter versus the actual pitch values.

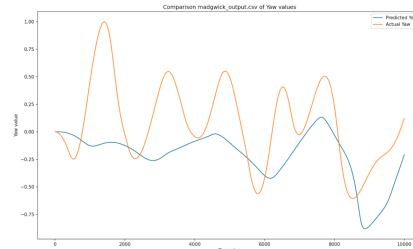


Fig. 12 Predicted yaw values of the Madgwick filter versus the actual yaw values.

As seen with Fig.10-12, Madgwick filter produced relatively accurate estimates that followed the magnitude and shape of the true trajectory.

VII. Mahony Filter

The Mahony filter also utilizes the complementary structure and is similar to the Madgwick filter in its calculations. The major differing factor would be its use of a proportional-integral (PI) feedback control. The filter starts with a state estimate, and the next time step is predicted with data from the gyroscopes. The estimate is then corrected with data from the accelerometer and magnetometer. A set of predicted sensor measurements is compared with the actual measurements, and the final estimate is adjusted accordingly. This filter's approach enables it to provide accurate and stable estimates of orientation even in the presence of external disturbances such as vibration or magnetic interference.[5]

The equation describing this system is:

$$q_t = q_{t-1} + \frac{1}{2} \hat{q} P (q_w + k_p \omega + k_i \int \omega) dt \quad (9)$$

Here, q_w represents the true angular velocity. The Mahony filter introduces two filter control parameters as per its PI used for error correction which makes it more flexible when compensating for drift in sensor readings. They are more commonly referred to as k_p and k_i instead of α_1 and α_2 [6] Here is the output of the Mahony filter compared to the actual trajectory.

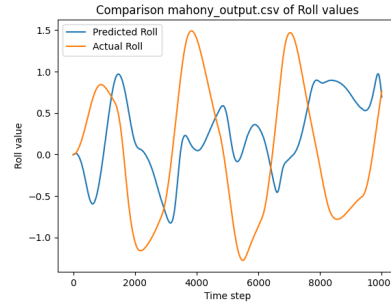


Fig. 13 Predicted roll values of the Mahony filter versus the actual roll values.

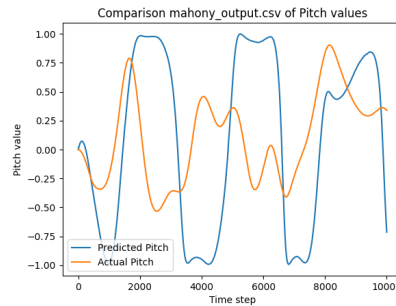


Fig. 14 Predicted pitch values of the Mahony filter versus the actual pitch values.

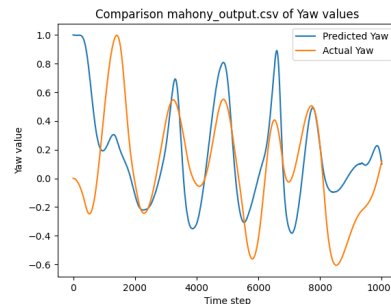


Fig. 15 Predicted yaw values of the Mahony filter versus the actual yaw values.

After analyzing the graphs that this filter produced, it ended up with the best estimation for the spiral trajectory's Yaw coordinates. As seen in Fig.15, the prediction and the actual Yaw values are closer together than any other filter.

VIII. Methodology

For this experiment, readings were generated for the nine-axis IMU to reflect a spiral trajectory. Furthermore, artificially introduced noise is used to simulate real-world conditions for the sensors. We then tuned each filter, if applicable, and proceeded to generate the algorithm's best estimate of the spiral trajectory. Each filter was evaluated by

their corresponding magnitudes of error in their roll, pitch, and yaw estimations. It is important to note that no singular measure of error provides an all-encompassing review of the filter. For attitude calculation, there is more concern about large values throwing off the accuracy of the filters, so the results of each filter are assessed by their root mean squared error (RMSE). When compared to the mean absolute error (MAE), the RMSE will give more weight to larger values being off from the prediction and give a more precise measurement of the filter performance.

IX. Results

Filters	Complementary	EKF	Fourati	Madgwick	Mahony
RMSE	2.7800	2.4498	1.4366	1.0431	1.3625

Table 1 RMSE of each filter.

Filters	Complementary	EKF	Fourati	Madgwick	Mahony
Roll RMSE	2.1716	1.8977	1.0314	0.8097	1.0104
Pitch RMSE	0.9224	0.9026	0.7901	0.4971	0.8230
Yaw RMSE	1.4701	1.2592	0.6129	0.4306	0.3976

Table 2 RMSE of Roll, Pitch, Yaw of each filter.

Table 1 displays the performances on the test readings given. The Madgwick filter performs most optimally for non-linear attitude estimation. This is followed by the Mahony, Fourati, EKF, and Complementary filters. To be more precise, the Madgwick filter was 267% more accurate than the worst-performing filter and 131% more accurate than the second-best-performing filter in our set.

Table 2 shows that the Madgwick filter performed the best amongst Roll and Pitch RMSEs, but was beaten by the Mahony filter when it came to the Yaw RMSE.

Looking back at the Complementary filter, the relatively poor performance does not discount its ability as an attitude estimator, but it is important to remember that one of its best qualities is its low computational burden. If a system were to value lower latency over the accuracy of its calculations, or a working system wants to be established without having to derive through complex math then the filter would be an ideal choice.

The Extended Kalman Filter, despite its heftier computations, did not perform as one may expect. This is less likely a descriptor of the validity of the algorithm but instead a careless tuning process. The EKF requires that the measurement and process noise covariance matrices Q and R are carefully tuned for a good performance. Referencing the outputs in Fig.4-6, the algorithm follows the general shape of the expected trajectory, but overshoots the points dictated by the true path which is one indication of necessary tuning[7].

While the results of Madgwick performing highest and Complementary being the least reliable is a consistent outcome among existing literature [8] [9], it is worth mentioning the possible room for error. Starting with the broader organization, this experiment contains design flaws as the filters were only tested on a singular case. There may be attributes about the trajectory that could cause one filter to perform slightly better than others and vice versa. Additionally, there were not tests for filters when it came to different magnitudes of noise being introduced to the data with a lack of unique test cases. Filters perform differently depending on how much noise is introduced to the readings, so to analyze if the outputs could be influenced by that, a variation of noise in test cases would be important too. Second, each filter was tuned for a variable amount of time meaning that it could be the case that better-performing filters were tuned better or poorly performing filters did not get proper tuning at all. This would account for the questionable performance of the EKF compared to the other filters despite its heavy computation. A redesign of this experiment should have these filters, tuned to their best performances and tested among a handful of sample sensor data and an array of different noise filters that can be introduced for each unique set of data.

X. Conclusion

In this paper, we present an experiment and comparison across various nonlinear filters and their accuracy when tuned, in predicting a predefined rocket path, we highlight some of the strengths and weaknesses within each, and we conclude that the Madgwick filter performed the best for our sampled trajectory, holding the smallest magnitude error. While each filter holds different specialties and benefits, for the time being, when considering the development of our Monoprop UAV and GNC testbeds, the Madgwick filter is the most likely one for integration. Its low magnitude of error and relatively inexpensive computational load is ideal for our use cases in progressing with our self-landing rocket. Picking a filter for our goal of achieving hovering, vertical take-off, and landing of a hybrid rocket, is not a one-time decision. Ultimately, as the development of the hybrid rocket continues and the state-space model is developed, a reevaluation of these algorithms would follow suit. This means analyzing the requirements and constraints of our hardware, noting which filters would be most effective for our goal, and tuning our finalized filter of choice to better reflect the sensor layout we include on the rocket.

Acknowledgments

As part of this project, we would like to express our gratitude to Propulsive Landers at Georgia Tech for providing us with the opportunity to conduct research as part of the organization's work.

References

- [1] Cavallo, A., "Experimental Comparison of Sensor Fusion Algorithms for Attitude Estimation," 2014, pp. 7585–7591. <https://doi.org/10.3182/20140824-6-ZA-1003.01173>.
- [2] Sabatini, A., "Quaternion-based extended Kalman filter for determining orientation by inertial and magnetic sensing," *IEEE Transactions on Biomedical Engineering*, Vol. 53, No. 7, 2006, pp. 1346–1356. <https://doi.org/10.1109/TBME.2006.875664>.
- [3] Fourati, H., Manamanni, N., Afilal, L., and Handrich, Y., "A Nonlinear Filtering Approach for the Attitude and Dynamic Body Acceleration Estimation Based on Inertial and Magnetic Sensors: Bio-Logging Application," *IEEE Sensors Journal*, Vol. 11, No. 1, 2011, pp. 233–244. <https://doi.org/10.1109/JSEN.2010.2053353>.
- [4] Madgwick, S., Harrison, A., and Vaidyanathan, R., "Estimation of IMU and MARG orientation using a gradient descent algorithm," *IEEE ... International Conference on Rehabilitation Robotics : [proceedings]*, Vol. 2011, 2011, p. 5975346. <https://doi.org/10.1109/ICORR.2011.5975346>.
- [5] Çoçoli, K., and Badia, L., "A Comparative Analysis of Sensor Fusion Algorithms for Miniature IMU Measurements," *2023 International Seminar on Intelligent Technology and Its Applications (ISITIA)*, 2023, pp. 239–244. <https://doi.org/10.1109/ISITIA59021.2023.10220994>.
- [6] Mahony, R., Hamel, T., and Pfimlin, J.-M., "Nonlinear Complementary Filters on the Special Orthogonal Group," *Automatic Control, IEEE Transactions on*, Vol. 53, 2008, pp. 1203 – 1218. <https://doi.org/10.1109/TAC.2008.923738>.
- [7] Zhang, A., and Atia, M. M., "An efficient tuning framework for Kalman filter parameter optimization using design of experiments and genetic algorithms," *NAVIGATION: Journal of the Institute of Navigation*, Vol. 67, No. 4, 2020, pp. 775–793. <https://doi.org/10.1002/navi.399>, URL <https://navi.ion.org/content/67/4/775>.
- [8] Parikh, D., Vohra, S., and Kaveshgar, M., "Comparison of Attitude Estimation Algorithms With IMU Under External Acceleration," 2022. <https://doi.org/10.1109/iSES52644.2021.00037>.
- [9] Capriglione, D., Carratù, M., Catelani, M., Ciani, L., Patrizi, G., Pietrosanto, A., and Sommella, P., "Experimental Analysis of Filtering Algorithms for IMU-Based Applications Under Vibrations," *IEEE Transactions on Instrumentation and Measurement*, Vol. 70, 2021, pp. 1–10. <https://doi.org/10.1109/TIM.2020.3044339>.